Journal of Materials Chemistry C

Accepted Manuscript

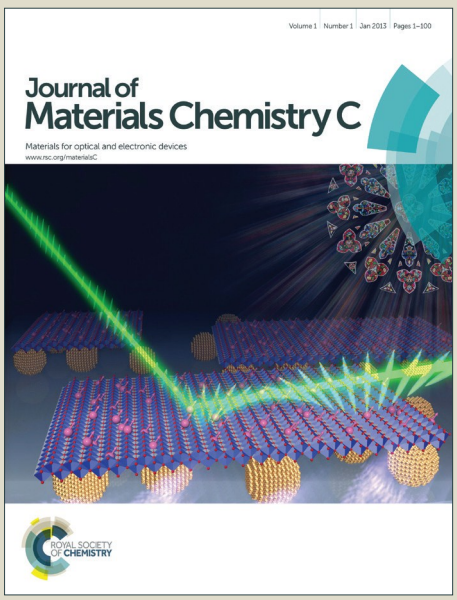

ROYAL SOCIETY OF CHEMISTRY

www.rsc.org/materialsC

Fluorescent nitrogen-rich carbon nanodots with an unexpected β-C_3N_4 nanocrystalline structure.

F. Messina[1], L. Sciortino[1], R. Popescu[2], A. M. Venezia[3], A. Sciortino[1,4], G. Buscarino[1], S. Agnello[1], R. Schneider[2], D. Gerthsen[2], M. Cannas[1], F. M. Gelardi[1]*

[1] Dipartimento di Fisica e Chimica, Università degli Studi di Palermo, Via Archirafi 36, 90123 Palermo, Italy

[2] Laboratory for Electron Microscopy, Karlsruhe Institute of Technology, Engesserstrasse 7, 76131 Karlsruhe, Germany

[3] Istituto per lo Studio dei Materiali Nanostrutturati, CNR, Via Ugo La Malfa, 153, 90146 Palermo, Italy.

[4] Dipartimento di Fisica ed Astronomia, Università degli Studi di Catania, Via Santa Sofia 64, 95123 Catania, Italy

Corresponding Author

*fabrizio.messina@unipa.it

Abstract:

Carbon nanodots are a class of nanoparticles with variable structures and compositions which exhibit a range of useful optical and photochemical properties. Since nitrogen doping is commonly used to enhance the fluorescence properties of carbon nanodots, understanding how nitrogen affects their structure, electronic properties and fluorescence mechanism, is important to fully unravel their potential. Here we use a multi-technique approach to study heavily nitrogen-doped carbon dots synthetized by a simple bottom-up approach, and capable of bright and color-tunable fluorescence in the visible. These experiments reveal a new variant of optically-active carbonaceous dots, that is a nanocrystal of beta carbon nitride (β-C_3N_4) capped by a disordered surface shell hosting a variety of polar functional groups. Because β-C_3N_4 is a network of sp^3 carbon and sp^2 nitrogen atoms, such a structure markedly contrast with the prevailing view of carbon nanodots as sp^2-carbon materials. The fluorescence mechanism of these nanoparticles is thoroughly analyzed and attributed to electronic transitions within a manifold of surface states associated to nitrogen-related groups. The sizeable bandgap of the β-C_3N_4 nanocrystalline core has an indirect, albeit important role in favoring an efficient emission. These results have deep implications on our current understanding of optically-active carbon-based nanoparticles and reveal the role of nitrogen in controlling their properties.

TOC entry

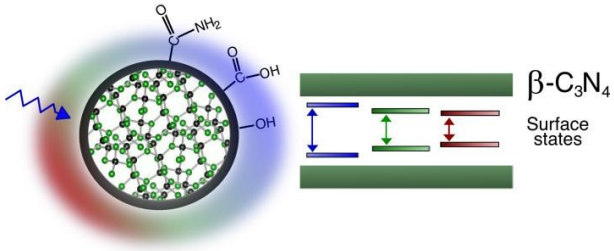

We report on nitrogen-doped carbon dots having a β-C_3N_4 crystalline structure and yielding a bright tunable fluorescence.

KEYWORDS: Nanocarbon, Carbon dots, Carbon nitride, fluorescent nanoparticles.

Introduction

Carbon nanodots (CDs) are a family of zero-dimensional (0D) nanomaterials consisting in carbonaceous nanoparticles smaller than 10 nm capable of bright and tunable fluorescence.[1-4] This property is mostly unparalleled by other carbon-based nanomaterials and, combined to water solubility, low toxicity, photo-stability, and a versatile photochemistry, has inspired a growing research interest in the last ten years,[5-6] in view of many applications such as bioimaging,[7-8] optoelectronics,[9-10] photocatalysis and solar energy harvesting.[11-12] CDs are indeed a rather broad family of nanomaterials with variable structures and compositions: beside carbon, they usually contain large amounts of oxygen (20-40%), especially at the surface, and nitrogen is often introduced as an additional dopant up to rather large concentrations.[13-16] While the core structure of CDs is mostly described as graphitic or turbostratic sp^2-carbon,[5-6] relatively few works provided clear evidence of a well-defined nanocrystalline graphitic core, exhibiting the characteristic (002) and (100) lattice spacings, 0.33 nm and 0.21 nm respectively.[2,4,17-18] Indeed, fluorescent CDs can also have amorphous cores,[19] and the ratio between sp^2 and sp^3 carbon atoms is variable from case to case.[5-6] The surface chemistry of CDs is equally complex, and mostly involves carboxylic and other polar groups which determine a large aqueous solubility.[1-6] Nitrogen-containing CDs (N-CDs) are particularly interesting because of their large fluorescence quantum yields,[13-15] but the reason of this is hardly understood so far. Rationalizing the structural variability of CDs, and understanding the relation between structure and optical properties are important and largely open problems in the field.

Indeed, also the mechanisms behind the efficient fluorescence of CDs and N-CDs are debated,[5-6] although it is generally agreed that very small sizes (typically < 5 nm) and an appropriate surface passivation are both needed for large quantum yields, resembling the behavior of traditional, metal-based semiconductor nanoparticles. Some works described the emission as a $\pi^* \rightarrow \pi$ transition of a quantum-confined sp^2 carbon core, based on the size-dependence of the emission color,[4,8,20] which resembles the optical properties of large aromatic molecules. Based on a recently proposed classification,[21] CDs controlled by this emission mechanism are characterized by well-defined crystalline structures and are named carbon quantum dots (CQDs), or graphene quantum dots in the particular case of a quasi-planar structure consisting in a few sheets of sp^2 carbon.[21] Many other authors, however, endorsed the idea that surface-localized states are responsible of the fluorescence of carbon dots,[1,13,18,22] as suggested by the decisive influence of surface passivation,[1,13,22-23] the sensitivity to solution pH,[3] and the ease by which photoexcited CDs behave as electron donors or acceptors.[24] In this case, the role of the small size would be to dramatically increase the surface-to-volume ratio, rather than inducing a quantum confinement effect on the core. This second emission mechanism is typical of CDs without a crystalline structure, named Carbon nanodots (CNDs),[21] although it can occur for CQDs as well. Notably, surface-localized states can be interpreted either as trap states inside a size-dependent bandgap, or as arising from individual surface emitters in the complete absence of collective effects. In any case, a certain distribution of sizes or of inequivalent surface chromophores is needed to explain the fluorescence tunability of CDs, that is the continuous change of the emission color with excitation wavelength.[1,3]

Here we report a careful study of the structural and electronic properties of highly fluorescent N-CDs synthetized by a simple bottom-up approach. We show the dots to have the unforeseen

core structure of a beta carbon nitride (β-C_3N_4) nanocrystal, a polymorph of C_3N_4 built from sp^3 carbon atoms bound to nitrogen. [25-27] We provide evidence that the emission of these N-CDs stems from a manifold of electronic states localized on the surface shell hosting a variety of polar functional groups terminating the β-C_3N_4 core. These results further expand the boundaries of the heterogeneous family of fluorescent carbon-based 0D systems, and contribute to clarify the role of nitrogen in controlling the structure and properties of N-CDs.

Experimental section

Sample preparation

We prepared N-CDs by thermally-induced decomposition of organic precursors, similarly to previous studies,[13-16] by the procedures hereafter described. A solution of P-CD (precursor of the carbon dots) is prepared by mixing citric acid monohydrate with urea (Sigma-Aldrich) in 10 mL of MilliQ water. In a typical synthesis, a volume of the P-CD solution is boiled up to the point where the complete evaporation of the solvent is observed. Hence, a dark material is collected. This latter, strongly hygroscopic, brought back to room temperature, is dried in vacuum for 90 minutes obtaining a fine black powder consisting of an aggregate of CDs. While N-CDs can be successfully synthesized throughout a wide range of molar ratios *R* between the organic acid and the source of nitrogen, the samples used in these experiments were all synthesized with *R*=0.28.

Characterization of N-CDs

Atomic force microscopy (AFM) images were acquired on a sample obtained by depositing a drop of an aqueous solution of N-CDs (0.05 g/L) on a mica substrate having subnanometer surface roughness. After drying in a vacuum environment for 2 hours, tapping-mode amplitude

modulation AFM measurements were performed by a Multimode V (Veeco Metrology) scanning probe microscope, equipped with a conventional piezoscanner (maximum xy range ≈14 μm and maximum z range ≈ 3.6 μm) and a four-segment photodetector for cantilever deflection monitoring. We used Pointprobe® Plus Silicon-SPM-probes with Al backside reflex coating, having a resonance frequency ≈300 KHz and a tip apical diameter of 5-10 nm. All the scans were executed at room temperature and in N_2 atmosphere, with a 2 nm/s tip velocity on the surface.

High-resolution transmission electron microscopy (HRTEM) was carried out on an aberration-corrected FEI Titan^3 80-300 microscope at 300 kV acceleration tension. The samples for TEM experiments were prepared on holey carbon-film copper-grids by deposition of as-prepared nanoparticles at room temperature in air. HRTEM images were evaluated by calculating their two-dimensional Fourier transform, denoted as diffractogram, which yields information on the crystal structure (lattice parameters and crystal symmetry) of single nanoparticles. The analysis was performed by comparing the experimental diffractograms to calculated diffraction patterns with Miller indices. The latter were obtained by using the JEMS (Java version of the electron microscopy simulation) software. The zero-order beam (ZB) is indicated on the diffractogram by using a white circle. Selected-area electron diffraction (SAED) patterns of nanoparticle ensembles were taken with a Philips CM 200 FEG/ST microscope at 200 kV, in order to investigate their crystal structure. Usually, SAED patterns of nanoparticles show only few and rather diffuse reflections on Debye-Scherrer rings. A way to prevent the loss of valuable diffraction information is the calculation of radially averaged SAED intensities (for short radial scans), which are obtained by a 2π integration of each spatial frequency $k = |\vec{k}|$ in the initial SAED pattern. Radial scans can be used to investigate the structure on nanoparticles similar to XRD patterns. Lattice parameters and crystal structure of nanoparticle material were determined

from radial scans by using the peak positions obtained by fitting a Voigt function to each individual peak profile after subtraction a linearly interpolated background.

Infrared (IR) absorption spectra were recorded at room temperature in transmission geometry on a N_2-purged Bruker spectrophotometer (model VERTEX-70) having a spectral resolution of 1 cm^{-1}. Sample powders were mixed with KBr and pressed to obtain a pellet. To eliminate the effect of residual water in air, the absorption spectrum of the KBr pellet was subtracted from the sample spectrum. X-ray photoelectron spectroscopy measurements were performed with a VG Microtech ESCA 3000 Multilab, equipped with a dual Mg/Al anode. The spectra were excited by the unmonochromatised Al Kα source (1486.6 eV) run at 14 kV and 15 mA. The analyzer operated in the constant analyser energy (CAE) mode. Survey spectra were measured at 50 eV pass energy. For the individual peak energy regions, a pass energy of 20 eV set across the hemispheres was used. The constant charging of the samples was corrected by referencing all the energies to the C 1s peak energy set at 285.1 eV, arising from adventitious carbon. Analyses of the peaks were performed with the software provided by VG, based on non-linear least squares fitting program using a weighted sum of Lorentzian and Gaussian component curves after background subtraction. The binding energy values are quoted with a precision of ± 0.15 eV and the atomic percentage with a precision of ± 10%.

Optical measurements

All optical measurements were carried out at room temperature in 1 cm quartz cuvettes. Steady-state optical absorption spectra of aqueous solutions (0.05 g/L) of N-CDs were recorded on a double beam spectrophotometer (JASCO V-560) operating in the 200-900 nm range (4.3-1.5 eV). Photoluminescence excitation (PLE) spectra were recorded by a JASCO FP6500

spectrofluorometer. The system is equipped with a 150 W Xenon lamp source and uses a photomultiplier as detector, operating in the range 4.1-1.8 eV. The spectrum of the lamp was measured using a concentrated solution of rhodamine B as a quantum counter, and used to correct the PLE spectra. We measured the photoluminescence quantum yield (QY) by comparing the steady-state emission intensity recorded from N-CDs in solution with that detected in a reference sample of known quantum yield (Fluorescein in H_2O @ pH=13, QY=0.95), both measured in a JASCO FP6500 spectrofluorometer in identical excitation and detection geometries. The reported QY are affected by an uncertainty of ±10% on the quoted values.

Time-resolved photoluminescence measurements were recorded on an intensified CCD camera while exciting the sample by a tunable laser system consisting in an optical parametric oscillator pumped by the third harmonic of a Nd:YAG laser (5 ns pulses at 10 Hz repetition rate). The CCD camera was electronically triggered to record the emission spectra in a definite time window (0.5 ns time resolution) with respect to laser pulses. The fluorescence spectra shown here were time-integrated in a window of 100 ns duration, delayed of ≈3-5 ns from the laser, and corrected for the response and dispersion of the detection system. The decay kinetics of the fluorescence were measured by recording spectra at variable delays from the laser pulse, and extracting the time dependence of the integrated emission intensity.

Results and Discussion

By the synthesis procedures described in the last section, we obtain a nanopowder which is easily dispersed in water and other polar solvents, forming stable solutions up to large concentrations (>15 g/L in H_2O). In contrast, the nanomaterial is virtually insoluble in weakly polar liquids.

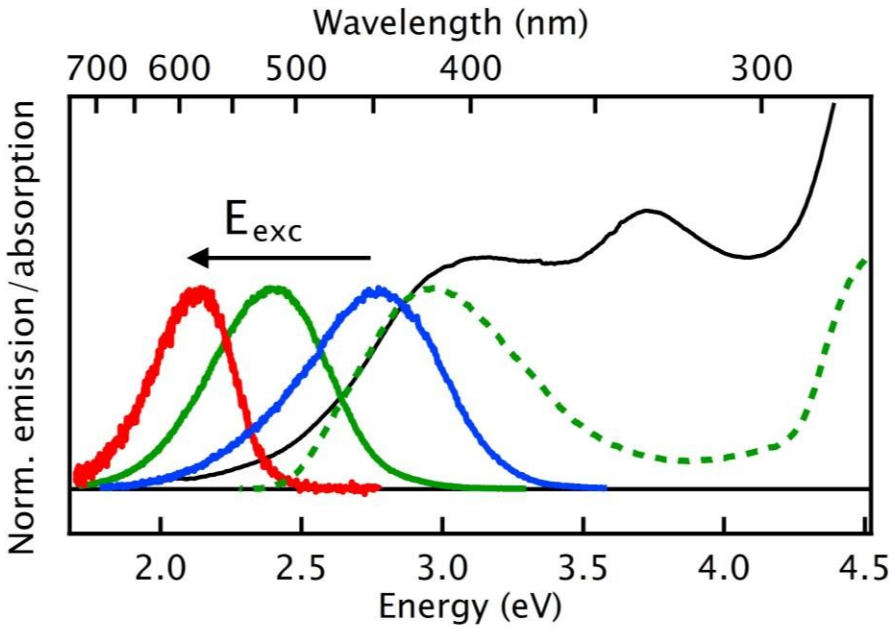

Figure 1. Normalized optical absorption spectrum (black line), fluorescence spectra excited at 3.5 (blue), 3.0 (green) and 2.3 eV (red), photoluminescence excitation spectrum of the green emission (green dashed line), as measured in a sample of N-CDs in aqueous solution (0.02 g/L).

Fig. 1 shows the optical absorption (OA) of N-CDs in water: the lowest-energy transition is a broad band peaking at 3.1 eV with an extended low-energy tail. An additional narrower band is

observed at 3.7 eV, and the OA coefficient steeply increases above 4.0 eV (see also Fig. S1 in the Supplementary information). The sample is strongly fluorescent when photo-excited from the deep-UV to the visible. The largest fluorescence intensity is observed (Fig. 1) when exciting around 3.0 eV, where we record a broad and unstructured emission at 2.4 eV with a quantum yield (QY) of η=0.12. The fluorescence redshifts continuously when decreasing the excitation energy, peaking at 2.8 eV, 2.4 eV, 2.1 eV when exciting at 3.5 eV, 3.0 eV, 2.3 eV, respectively (Fig. 1). The lifetime (Fig. S2) ranges from 4 to 7 ns depending on the excitation energy. Combined with the large QY, these values imply radiative lifetimes of a few tens of ns, which signifies strongly dipole-allowed electronic transitions. All these properties are rather characteristic of carbonaceous dots, especially the excitation-dependent tunability of the fluorescence.[1-6]

Atomic force microscopy (AFM, Figs. 2 and S3) and high-resolution transmission electron microscopy (HRTEM, Figs. 2 and S4) reveal that the material consists of isolated nanoparticles, that is, N-CDs. X-ray photoelectron spectroscopy (XPS, see Fig. S5) confirms rather large nitrogen and oxygen contents, common for fluorescent N-CDs. The distribution of topographic heights obtained by AFM is shown in Fig. 2a and indicates an average diameter of 3 nm. HRTEM confirms this view by showing many N-CDs with typical sizes of ≈3 nm (Fig. S4). More importantly, lattice fringes extend through the whole particle core, as visible on the HRTEM image of a representative single dot (Fig. 2b), and demonstrate its crystalline structure. Indeed, these HRTEM images indicate that the N-CD core is a single mono-crystal of β-C_3N_4, as suggested by the good agreement between its diffractogram (Fig. 2c) and the calculated diffraction pattern of hexagonal β-C_3N_4 (space group $P6_3/m$, space group number 176, with a=6.380 Å and c=2.395 Å, as from ref.[26]) in the [310]-zone axis.

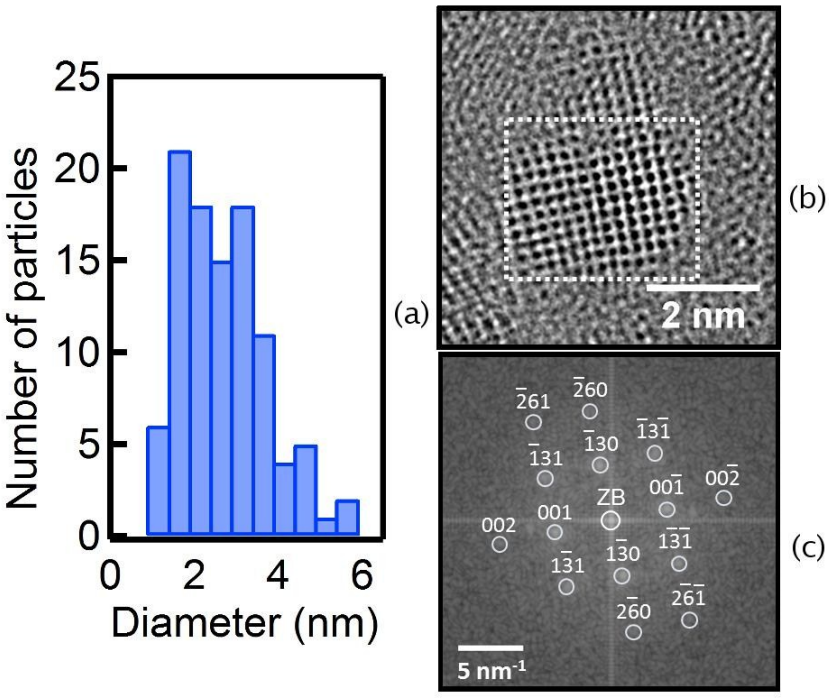

Figure 2. Size distribution of N-CDs measured by AFM. b) HRTEM image of a single N-CD and c) experimental diffractogram of the nanoparticle shown in b) and calculated diffraction pattern with Miller indices for hexagonal bulk β-C_3N_4 in the [310]-zone axis (blue circles). The central spot indicates the zero-order beam (ZB).

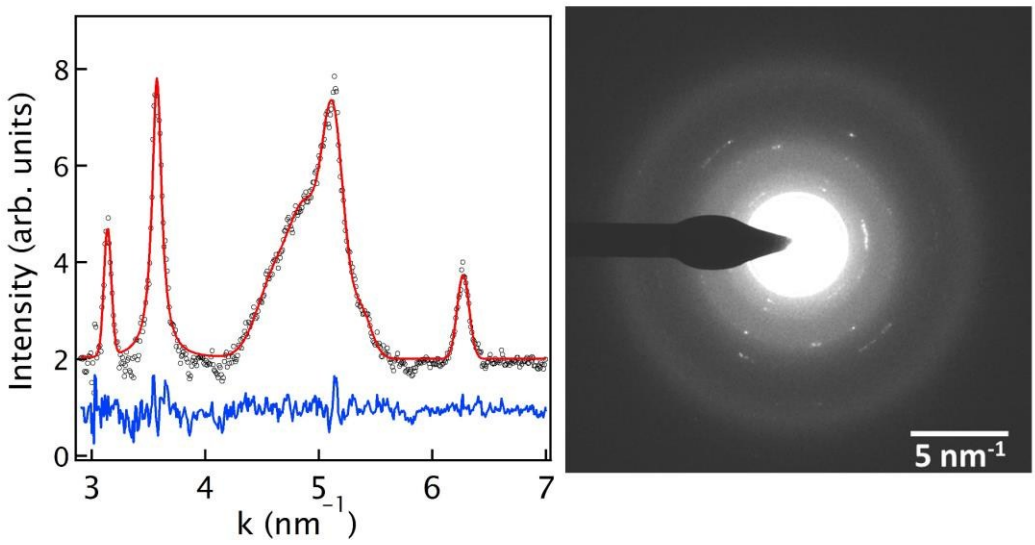

Figure 3. Right panel: SAED pattern of N-CDs. Left panel: radial scan of the SAED pattern (open symbols), whole-pattern fit (red line) and residuals (blue line) used for the structure analysis.

We obtain further, accurate structural information on N-CDs from selected-area electron diffraction (SAED) measurements, as shown in Fig. 3. The position of each diffraction line of the radial scan is determined by fitting a Voigt function to its individual profile, after subtracting a linear interpolated background. As a result, all observed Debye-Scherrer rings can be assigned to hexagonal β-C_3N_4, confirming the HRTEM results. The peak positions (Table S1) in the radial scan result in lattice parameters of a=6.37±0.06 Å and c=2.40±0.02 Å for the hexagonal β-C_3N_4 structure of N-CDs. The lattice parameters we find here from SAED closely agree to previous XRD[28-29] and electron diffraction data[30-31] obtained from nanosized β-C_3N_4, and to theoretical predictions,[26] although both the peak broadening in SAED measurements and a certain dot-to-dot

fluctuation of lattice parameters in HRTEM images indicate significant strains in the lattice structures of these β-C_3N_4 dots.

Based on the literature, crystals with a C_3N_4 stoichiometry occur in graphitic (g-C_3N_4), cubic (γ-C_3N_4) and hexagonal (α-C_3N_4 and β-C_3N_4) phases.[26-35] While g-C_3N_4 is considered the most stable polymorph of carbon nitride,[33-34] recent theoretical studies suggest β-C_3N_4 to be favored below a certain threshold size.[27] However, relatively a few experiments reported the successful synthesis of nanosized β-C_3N_4,[28-32] ideally consisting in a hexagonal network of tetrahedral bonded (sp^3) C atoms connected to trigonal (sp^2) nitrogen atoms. In regard to fluorescent CDs, in the literature they are mostly looked at as sp^2-carbon nanomaterials,[1-6] although only a few HRTEM studies clearly proved them to have the crystalline structure of graphite.[2,4,17-18] When CDs are doped with Nitrogen, their surfaces usually host plentiful amide and amine moieties,[13-15] but in some cases nitrogen is also found in the core as a structural dopant.[13] Based on this, one may expect large concentrations of nitrogen to alter the very crystalline structure of the dot. In fact, recent studies found highly N-doped, fluorescent CDs to host a graphitic carbon nitride (g-C_3N_4) core lattice.[36-39] g-C_3N_4 is a layered structure of sp^2 carbon and nitrogen,[33-34] whose aromatic planes are built from tri-s-triazine units connected by amino groups. However, g-C_3N_4 is again a sp^2 carbon material, quite different from the β-C_3N_4 core structure we found here, built from sp^3-carbon and sp^2-nitrogen. β-C_3N_4 dots are also obviously different from nanodiamonds,[40] which have almost pure sp^3-carbon cores associated to very large (>5 eV) electronic bandgaps, and emit luminescence only in the presence of point defects, yielding comparatively narrow emission with well-defined and non-tunable spectral features.[5,40] Thus, the present evidence of highly fluorescent N-CDs with a β-C_3N_4 core, and the behavior of β-C_3N_4

nanocrystals as efficient emitters, are rather unanticipated by the literature, despite many studies synthesized CDs with similar procedures.[13-16]

We used Fourier-Transform Infrared absorption (FTIR) and X-ray Photoelectron Spectroscopy (XPS) to further study N-CDs. The main mid-IR absorption peaks (Fig. 4) appear at 1401, 1622, 1671 and 1716 cm^{-1}. The C-N stretching vibration in both α– and β–C_3N_4 gives rise to a sharp phonon mode around 1380 cm^{-1},[32,41] while theoretical calculations find the highest-frequency IR-active mode of β-C_3N_4 at 1328 cm^{-1}.[26] Hence we attribute the peak at 1401 cm^{-1} to a C-N vibration within the β-C_3N_4 nanocrystals. The absorption beyond 1500 cm^{-1} stems from a variety of surface groups decorating the β-C_3N_4 cores. Based on the literature,[13-15] we attribute the peaks at 1622 and 1671 cm^{-1} to amide (amide I and II modes) and the peak at 1716 cm^{-1} to carboxylic moieties. The sample also displays a complex absorption (Fig. S6) between 2600 and 3600 cm^{-1} due to O-H, N-H, and possibly C-H stretching vibrations.

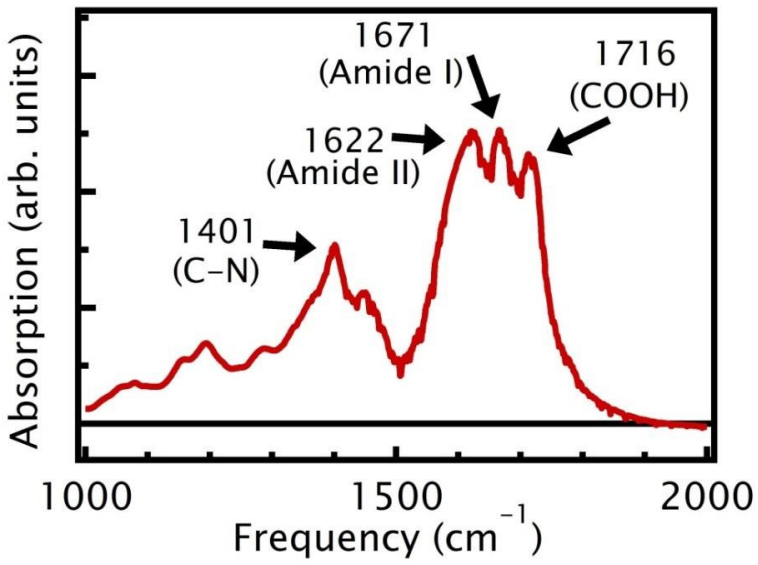

Figure 4. Mid-IR absorption spectrum of N-CDs. The arrows highlight our attributions of the signals, as discussed in more detail in the text.

In XPS measurements, the C_{1s} signal (Fig. 5) contains a large contribution at 285.1 eV due to C-C and C-H bonds (hereafter referred to as C_0). This mostly arises from hydrocarbon contamination of the sample chamber (and possibly to some surface C-C and C-H bonds). Beside the C_0 signal, a high-resolution scan reveals two more contributions at 287.7 eV and 288.8 eV. The former (C_{core}=287.7 eV) is due to sp^3–type C-N bonds within the β-C_3N_4 core, in very close agreement (within 0.2 eV) with previously reported XPS data for β-C_3N_4.[29,32] We ascribe the peak at 288.8 eV (C_{II}) to surface C atoms bound to oxygen (C=O) in carboxylic or amide moieties.

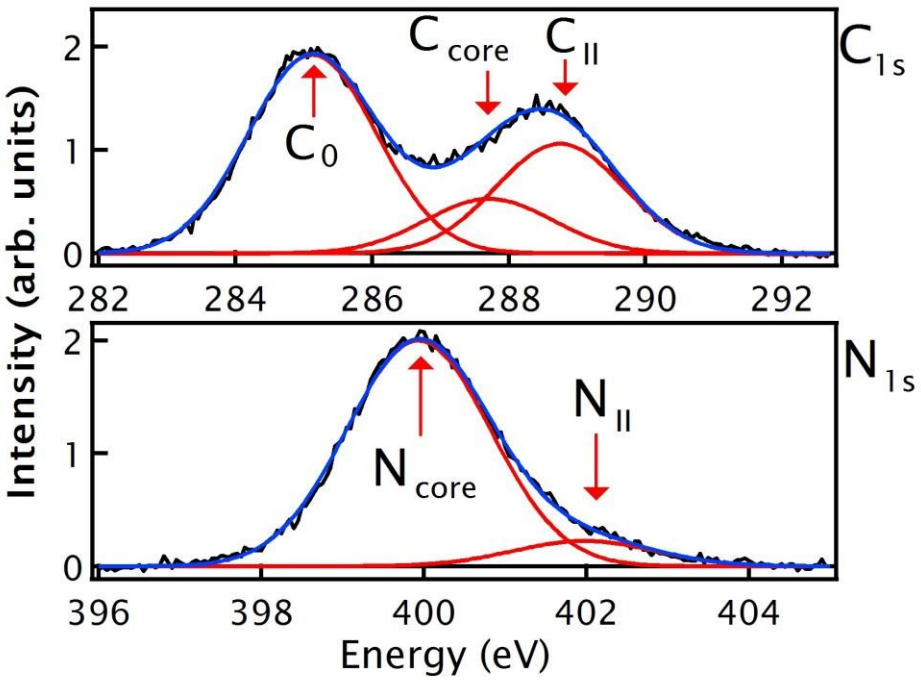

Figure 5. XPS C_{1s}, and N_{1s} signals detected in N-CDs (black lines), their decomposition in different contributions, described in the text (red lines), and the resulting fits of the experimental data (blue lines).

The N_{1s} signal contains two contributions at 399.9 eV and 401.9 eV. We attribute the former (N_{core}=399.9 eV) to N atoms belonging to the β-C_3N_4 core, originating from nitrogen atoms in trigonal geometry (sp^2). Notably, the atomic ratio N_{core}/C_{core}, as derived from the experimental XPS intensity ratio, equals 1.40, close to the expected value of 1.33 expected for a C_3N_4 stoichiometry. The additional, minor N_{II} =401.9 eV contribution likely derives from surface protonated nitrogen of amide or N-O bonds.[42] Finally, the O_{1s} signal (Fig. S7) contains contributions at 531.6 eV and 533.4 eV, due to carboxylic/amide oxygen atoms, and to hydroxyl groups respectively. Summarizing the results of Figs. 2-5 and S3-S7, these fluorescent dots consist in β-C_3N_4 nanocrystals capped by a disordered surface layer hosting amide, carboxylic, and hydroxyl moieties, all quite common on N-CDs surfaces.[13-15] One should also stress that the functional groups revealed by XPS and FTIR may partly arise from core defects, in addition to surface moieties.

We discuss now the fluorescence mechanism of these N-CDs. From the electronic point of view C_3N_4 polymorphs are semiconductors, inherently compatible with a visible fluorescence. In particular, g-C_3N_4 materials are photoluminescent[43] and photochemically active,[34] consistent with a bandgap of 2.0-2.5 eV.[27,34] As for β-C_3N_4, quantum chemical calculations estimate its bulk bandgap as 3.27 eV,[27] possibly increasing to >4 eV for nanosized systems. Hence, band-to-band transitions in the β-C_3N_4 core of N-CDs likely explain the steep increase of the OA at energies > 4 eV (Fig. 1 and Fig. S1) but hardly the absorption band at 3.1 eV with its extended low-energy tail, where an intense fluorescence can still be excited well below 2.5 eV (see Fig. 1). This strongly suggests that the lowest-energy transitions of N-CDs, responsible of the fluorescence, involve mid-gap electronic states. A typical photoluminescence excitation spectrum (PLE) singles out a well-defined band out of the OA spectrum. For instance (Fig. 1) the

PLE of the emission at 2.4 eV appears as a band at 2.96 eV, roughly mirror-symmetric to the emission, and accounting for most of the first OA band at 3.1 eV. This implies again that the fluorescence is "molecular-like", in that it occurs across a pair of mid-gap, localized electronic states isolated in the energy spectrum of the system, rather than involving band-to-band excitation. Interestingly, we measured a reduction of the QY for deep-UV excitations (e.g. η=0.04 exciting at 4.3 eV), suggesting a different excitation-emission pathway initiated by direct excitation across the β-C_3N_4 core bandgap. In general, midgap localized states in a nanocrystal are associated either to the surface or to core point defects. To discriminate between the two possibilities, we studied how the fluorescence is affected by the solvent and by the presence of metal ions in solution. In this respect, we found that: (a) metal ions (Cu^{2+}, Ag^{+}) efficiently quench the fluorescence (Fig. S8), suggesting significant overlap between the emitting states and the aqueous ions (b) The QY of N-CDs in D_2O is twofold larger than in H_2O (Fig. S9) and the QY is systematically larger in aprotic solvents as compared to protic solvents **(**Fig. S10**)**, highlighting that the fluorescence is deeply affected by short-range hydrogen bonding between the surface of N-CDs and the solvent and, possibly, by the occurrence of hydrogen-deuterium exchange on superficial groups. These two findings strongly point to the surface model, in that they show that the emissive electronic states are intensely coupled to the environment. Because the fluorescence is essentially related to the surface shell, it is not surprising that the emission properties of β-C_3N_4 dots overall resemble other types of CDs. [5,6]

The emission tunability of N-CDs highlights that the HOMO-LUMO gaps of the emitters are inhomogeneously distributed (roughly from ~2.0 eV to ~3.5 eV) and selected by the excitation energy. This is a disorder-related effect due to different local environments around the chromophore and/or to the involvement of multiple types of chromophores. This overall energy

manifold of midgap states gives rise to the broad OA band at 3.1 eV, whose inverse transitions produce a tunable fluorescence. Ascribing CD fluorescence to surface states is widespread independently of their core structure.[1,13,18,22] Here we propose that the relatively large core bandgap of β-C_3N_4 indirectly favors an efficient surface emission, hence a large QY, because surface emission would tend to be quenched by energy transfer towards a small-bandgap core. Because graphite has essentially a zero bandgap, CDs with a purely graphitic core (i.e. without N-doping) can only acquire a sizeable bandgap via a quantum confinement mechanism, if their size is small enough (bandgap >2 eV requires sizes of ≈1 nm or smaller[44]). In contrast, the bandgap of C_3N_4 polymorphs is > 2 eV already in the bulk form, [27,34] such that no quantum confinement needs to be invoked to explain the emission. Indeed, the role of the nanometric size for β-C_3N_4 dots is probably just a substantial increase of the surface-to-volume ratio, hence a high density of emitting states. In this sense, based on the accepted classifications these β-C_3N_4 dots should be pictured as carbon nanodots (CNDs) rather than truly "quantum" dots (CQDs).[21]

In the literature, CDs seldom display well-defined OA bands at energies as low as the lowest-energy peak found here (Fig. 1). Such low-lying transitions were mostly reported for N-CDs,[10,15] and were previously attributed to their N-functionalized surfaces.[10] Combining this with present FTIR and XPS results suggests that the emitting transitions of these β-C_3N_4 dots involve surface N-related groups, and especially amide moieties, although further studies are needed to pinpoint the precise structure of the emitting chromophore.

Conclusions

In this work we studied the structure and optical properties of 3 nm-sized, heavily nitrogen-doped carbon dots, synthesized by carbonization of citric acid and urea, a synthesis route close to

previous literature reports. Careful analysis of HRTEM images and SAED patterns, combined to AFM, XPS and FTIR, revealed that these dots consist in a monocrystal of beta carbon nitride surrounded by a disordered shell hosting a variety of polar functional groups. Such results underscore the role of heavy nitrogen doping in altering the very crystalline structure of carbon dots, a fact which is unexplored in the existing literature and bears relevant consequences on their electronic properties. Interestingly, the β-C_3N_4 core of these dots is built from sp^3 carbon atoms bound to sp^2 nitrogen, in sharp contrast with the prevailing view of CDs as a nanomaterial with a graphitic-derived structure. The wide electronic bandgap of β-C_3N_4 favors an efficient fluorescence, which provides an interpretation of the so-far elusive capability of nitrogen doping of increasing the emission quantum yield of CDs. On the other hand, the emission mechanism of these dots is mostly controlled by surface-localized electronic transitions, as inferred by the spectral range where the fluorescence can be efficiently excited, and by its sensitivity to the solvent and to the presence of metal ions in solution. Beside providing insight on the emission mechanism, the sensitivity to metal ions and to the solvent appear promising for sensing applications, to be fully investigated by further studies. Overall, the results reveal surface-functionalized β-C_3N_4 nanocrystals as a new class of optically-active 0D carbonaceous nanosystems, advancing our present knowledge of the eclectic family of CDs.

Acknowledgements

We thank the LAMP group (www.unipa.it/lamp) for support and scientific discussions. This research received support from the QualityNano Project http://www.qualitynano.eu/ financed by European Community Research Infrastructure Action under the FP7 "Capacities" Program."

References

(1) Y.-P. Sun, B. Zhou, Y. Lin, W. Wang, K. A. Shiral Fernando, P. Pathak, M. J. Meziani, B. A. Harruff, X. Wang, *et al.* Quantum-Sized Carbon Dots for Bright and Colorful Photoluminescence. *J. Amer. Chem. Soc.* 2006, **128**, 7756-7757.

(2) J. G. Zhou, C. Booker, R. Y. Li, X. T. Zhou, T. Sham, X. Sun, Z. Ding, An Electrochemical Avenue to Blue Luminescent Nanocrystals from Multiwalled Carbon Nanotubes (MWCNTs). *J. Am. Chem. Soc.* 2007, **129**, 744-745.

(3) D. Pan, J. Zhang, Z. Li, C. Wu, X. Yan, M. Wu, Observation of pH-, solvent-, spin-, and excitation-dependent blue photoluminescence from carbon nanoparticles. *Chem. Commun.* 2010, **46**, 3681-3683.

(4) H. Li, X. He, Z. Kang, H. Huang, Y. Liu, J. Liu, S. Lian, C. H. A. Tsang, X. Yang, S.-T. Lee, Water-Soluble Fluorescent Carbon Quantum Dots and Photocatalyst Design. *Angew. Chem. Int. Ed.* 2012, **49**, 4430–4434.

(5) S. N. Baker, G. A. Baker, Luminescent Carbon Nanodots: Emergent Nanolights. *Angew. Chem. Int. Ed.* 2010, **49**, 6726-6744.

(6) H. Li, Z. Kang, Y. Liu, S.-T. Lee, Carbon nanodots: synthesis, properties and applications. *J. Mater. Chem.* 2012, **46**, 24175-24478.

(7) S. C. Ray, A. Saha, N. R. Jana, R. Sarkar, Fluorescent Carbon Nanoparticles: Synthesis, Characterization, and Bioimaging Application. *J. Phys. Chem. C.* 2009, **113**, 18546-18551.

(8) S. K. Bhunia, A. Saha, A. R. Maity, S. C. Ray, N. R. Jana, Carbon Nanoparticle-based Fluorescent Bioimaging Probes. *Scientific Reports* 2013, **3**, 1473.

(9) F. Wang, Y.-H. Chen, C.-Y. Liu, D.-G. Ma, White light-emitting devices based on carbon dots'electroluminescence. *Chem. Commun.* 2011, **47**, 3502-3504.

(10) X. Zhang, Y. Zhang, Y. Wang, S. Kalytchuk, S. V. Kershaw, Y. Wang, P. Wang, T. Zhang, Y. Zhao, H. Zhang *et al.* Color-Switchable Electroluminescence of Carbon Dot Light-Emitting Diodes. *ACS Nano* 2013, **7**, 11234-11241.

(11) P. Mirtchev, E. J. Henderson, N. Solheilnia, C. M. Yip, G. A. Ozin, Solution phase synthesis of carbon quantum dots as sensitizers for nanocrystalline TiO_2 solar cells. *J. Mater. Chem.* 2012, **22**, 1265-1269.

(12) X. Yu, J. Liu, Y. Yu, S. Zuo, B. Li, Preparation and visible light photocatalytic activity of carbon quantum dots/TiO_2 nanosheet composites. *Carbon* 2014, **68**, 718-724.

(13) X. Zhai, P. Zhang, C. Liu, T. Bai, W. Li, L. Dai, W. Liu, Highly luminescent carbon nanodots by microwave-assisted pyrolysis. *Chem. Commun.* 2012, **48**, 7955-7957.

(14) M. J. Krysmann, A. Kelarakis, P. Dallas, E. P. Giannelis, Formation Mechanism of Carbogenic Nanoparticles with Dual Photoluminescence Emission. *J. Amer. Chem. Soc.* 2012, **134**, 747-750.

(15) S. Qu, X. Wang, Q. Lu, X. Liu, L. Wang, A Biocompatible Fluorescent Ink Based on Water-Soluble Luminescent Carbon Nanodots. *Angew Chem. Int. Ed.* 2012, **51**, 12215-12218.

(16) F. Messina, L. Sciortino, G. Buscarino, S. Agnello, F. Gelardi, M. Cannas, Photoluminescence of carbon dots embedded in a SiO_2 matrix, *Mater. Today Proceedings* 2015, in press.

(17) Z.-Q. Xu, L.-Y. Yang, X.-Y. Fan, J.-C. Jin, J. Mei, W. Peng, F.-L. Jiang, Q. Xian, Y. Liu, Low temperature synthesis of highly stable phosphate functionalized two color carbon nanodots and their application in cell imaging. *Carbon* 2014, **66**, 351-360.

(18) K. Linehan, H. Doyle, Efficient one-pot synthesis of highly monodisperse carbon quantum dots. *RSC Adv.* 2014, **4**, 18-21.

(19) S. Zhu, Q. Meng, L. Wang, J. Zhang, Y. Song, H. Jin, K. Zhang, H. Sun, H. Wang, B. Yang, Highly Photoluminescent Carbon Dots for Multicolor Patterning, Sensors, and Bioimaging. *Angew. Chem. Int. Ed.* 2013, **125**, 4045-4049.

(20) R. Ye, C. Xiang, J. Lin, Z. Peng, Z. Huanh, K. Yan, N. P. Cook, E. L. G. Samuel, C.-C.-Hwang, G. Ruan, A.-R. O. Ceriotti, G. Raji, A. A. Martì, J. M. Tour, Coal as an abundant source of graphene quantum dots. *Nat. Commun.* 2013, **4**, 2943.

(21) A. Cayuela, M. L. Soriano, C. Carrillo-Carriòn, M. Valcarcel, Semiconductor and carbon-based fluorescent nanodots: the need for consistency. *Chem. Commun.* 2016, **52**, 1311.

(22) Y. Liu, C.-Y. Liu, Z.-Y. Zhang, Synthesis and surface photochemistry of graphitized carbon quantum dots. *J. Colloid Interface Sci.* 2011, ***356***, 416-421.

(23) A. Cayuela, M. L. Soriano, M. Valcárcel, Strong luminescence of Carbon Dots induced by acetone passivation: Efficient sensor for a rapid analysis of two different pollutants. *Anal. Chim. Acta* 2013, **804**, 246-251.

(24) X. Wang, L. Cao, F. Lu, M. J. Meziani, H. Li, G. Qi, B. Zhou, B. A. Harruff, F. Kermarrec, Y.-P. Sun, Photoinduced electron transfers with carbon dots. *Chem. Commun.* 2009, 3774-3776.

(25) A. Y. Liu, M. L. Cohen, Prediction of New Low Compressibility Solids. *Science* 1989, **245**, 841-842.

(26) M. Marqués, J. Osorio, R. Ahuja, M. Florez, J. M. Recio Pressure effects on the structure and vibrations of β and γ-C_3N_4. *Phys. Rev. B* 2004, **70**, 104114.

(27) J. Luo, B. Wen, R. Melnik, Relative stability of nanosized β-C_3N_4 and graphitic C_3N_4 from first principle calculations. *Physica E* 2012, **45**, 190-193.

(28) D. W. He, F. X. Zhang, X. Y. Zhang, Z. C. Qin, M. Zhang, R. P. Liu, Y. F. Xu, W. K. Wang, Synthesis of carbon nitride crystals at high pressures and temperatures *J. Mater. Res.* 1998, **13**, 3458-3462.

(29) Q. Lv, C. Cao, C. Li, J. Zhang, H. Zhu, X. Kong, X. Duan, Formation of crystalline carbon nitride powder by a mild solvothermal method. *J. Mater. Chem.* 2003, **13**, 1241-1243.

(30) Y.-A. Li, S. Xu, H.-S. Li, W.-L. Luo, Polycrystalline carbon nitride β-C_3N_4 films synthesized by radio frequency magnetron sputtering *J. Mater. Sci. Letters* 1998, **17**, 31-35.

(31) L.-W. Yin, Y. Bando, M.-S. Li, Y.-X. Liu, Y.-X, Qi, Unique Single-Crystalline Beta Carbon Nitride Nanorods. *Adv. Mater.* 2003, **15**, 1840-1844.

(32) L.-W. Yin, M.-S. Li, G. Luo, J.-L. Sui, J.-M. Wang, Nanosized beta carbon nitride crystal through mechanochemical reaction. *Chem. Phys. Lett.* 2003, **369**, 483-489.

(33) L. Fang, H. Ohfuji, T. Shinmei, T. Irifune, Experimental study on the stability of graphitic C_3N_4 under high pressure and high temperature. *Diam. Relat. Mater.* 2011, **20**, 819-825.

(34) X. Wang, K. Maeda, A. Thomas, K. Takanabe, G. Xin, J. M. Carlsson, K. Domen, M. Antonietti, A metal-free polymeric photocatalyst for hydrogen production from water under visible light. *Nat. Mater.* 2009, **8**, 76-80.

(35) E. Kroke, M. Schwarz, Novel group 14 Nitrides. *Coord. Chem. Rev.* 2004, **248**, 493-532.

(36) S. Barman, M. J. Sadhukhan, Facile bulk production of highly blue fluorescent graphitic carbon nitride quantum dots and their application as highly selective and sensitive sensors for the detection of mercuric and iodide ions in aqueous media. *J. Mater. Chem.* 2012, **22**, 21832-21837.

(37) S. Liu, J. Tian, L. Wang, Y. Luo, X. Sun, A general strategy for the production of photoluminescent carbon nitride dots from organic amines and their application as novel peroxidase-like catalysts for colorimetric detection of H_2O_2 and glucose. *RSC Advances* 2012, **2**, 411-413.

(38) J. Zhou, Y. Yang, C.-Y. Zhang, A low-temperature solid-phase method to synthesize highly fluorescent carbon nitride dots with tunable emission. *Chem. Commun.* 2013, **49**, 8605-8607.

(39) S. Zhang, J. Li, M. Zeng, J. Xu, X. Wang, W. Hu, Polymer nanodots of graphitic carbon nitride as effective fluorescent probes for the detection of Fe^{3+} and Cu^{2+} ions. *Nanoscale* 2014, **6**, 4157-4162;

(40) S.-J. Yu, M.-W. Kang, H.-C. Chang, K.-M. Chen, Y.-C. Yu, Bright Fluorescent Nanodiamonds: No Photobleaching and Low Cytotoxicity. *J. Am. Chem. Soc.* 2005, **127**, 17604-17605.

(41) X. Bai, C. Cao, X. Xu, Q. Yu, Synthesis and characterization of crystalline carbon nitride nanowires. *Solid State Commun.* 2010, **150**, 2148-2153.

(42) D. Marton, K. J. Boyd, A. H. Al-Bayati, S. S. Todorov, J. W. Rabalais, Carbon Nitride Deposited Using Energetic Species: A Two-Phase System. *Phys. Rev. Lett.* 1994, **73**, 118-121.

(43) J. Xu, M. Shalom, F. Piersimoni, M. Antonietti, D. Neher, T. J. K. Brenner, Color-tunable Photoluminescence and NIR electroluminescence in Carbon Nitride thin films and Light-Emitting Diodes, *Adv. Opt. Mater.* 2015, **3**, 913-917.

(44) G . Eda, Y.-Y. Lin, C. Mattevi, H. Yamaguchi, H.-A. Chen, I.-S. Chen, C.-W. Chen, M. Chowalla, Blue Luminescence from chemically derived graphene oxide. *Adv. Mater.* 2010, **22**, 505-509.